An Event-Triggered Model Predictive Control for Energy Efficiency and Thermal Comfort Optimization in Buildings

Yang Shiyu[1], **Chen Wanyu**[2] **and Wan Man Pun**[2]

[1]Energy Research Institute at NTU, Nanyang Technological University, Singapore 637553
[2]School of Mechanical and Aerospace Engineering, Nanyang Technological University, Singapore 639798

Corresponding author mpwan@ntu.edu.sg

Abstract. Model predictive control (MPC) is a promising optimal control technique for building automation. However, the high computation load to solve the optimization problem of MPC is challenging its implementation for real-time building control. Typical MPC systems employ the time-triggered mechanism (TTM), which conducts the optimization periodically at each control interval regardless of the necessity. This study proposes an event-triggered mechanism (ETM) for MPC, which conducts the optimization only when there is a triggering event that necessitates it. Contrasting to the conventional ETM that bases only on the current information, the proposed ETM bases on the cost function considering the past, current and future information. An event-triggered model predictive control (ETMPC) system is developed using the proposed ETM. In a simulation environment, the ETMPC system is implemented to control an air-conditioning system. The ETMPC is compared to a MPC employing TTM and a conventional thermostat. The ETMPC improved the computation efficiency by 77.6% - 88.2% as compared to the MPC while achieving similar energy performance as the MPC does (both achieved more than 9% energy savings over the thermostat). The ETMPC only degraded the thermal comfort performance slightly as compared to the MPC but is still much better than the thermostat.

Keyword. Model Predictive Control; Event Triggered Mechanism; Air Conditioning and Mechanical Ventilation; Thermal Comfort; Building Automation and Control

1.Introduction

Improving energy efficiency is one of the most cost-effective approaches for meeting the growing energy demand and mitigating the increasing carbon emissions worldwide [1]. Studies suggest that the building sector has large potential for cost-effective improvement in energy efficiency and reduction of carbon emissions [2]. Buildings consume up to 40% of global final energy [3] and most energy use in buildings is attributed to building service systems (e.g., heating, ventilation, and air conditioning (HVAC) systems or air-conditioning and mechanical ventilation (ACMV) systems, lighting, etc.) [4]. Hence, much research efforts have focused on optimizing the operation of HVAC/ACMV systems through advanced control techniques for improving building energy efficiency. One of the most successful advanced control techniques is model predictive control (MPC), which has been demonstrated capable of achieving substantial energy savings and improved occupant's well-being for buildings in many previous studies.

MPC foresees the future building responses (e.g., indoor thermal comfort) by exploiting a mathematical model of the building as well as forecasted/measured disturbances (e.g., weather conditions and internal heat loads) and, subsequently, searches for optimal control strategies by taking the future building responses into consideration. However, a major technological barrier prohibiting the wide application of MPC for real buildings is the high computational power required to solve its optimization problem. One of the key factors leading to the high computation load of MPC is the complexity of building models. This has been addressed in many previous studies by simplifying building models through linear building modelling [5][6] or online building model linearization [7]. Another key factor is the receding horizon principle of MPC, which conducts the optimization

periodically to update the control strategies at each time step (control interval of MPC) regardless of the necessity of optimization in each of the time steps. This time-triggered mechanism (TTM) of optimization in MPC could lead to redundant optimizations, wasting computational power unnecessarily. A possible solution to this issue is to replace the TTM with an event-triggered mechanism (ETM) into MPC to form an event-triggered MPC (ETMPC), which only conducts the optimization when it is needed, i.e., a triggering event is detected.

A few previous studies employed the ETM control approaches for buildings. Most of these previous studies incorporated ETM into the Markov Decision Process (MPD) framework to establish the 'event-policy-action' structure, i.e. mapping from the event space (a set of events) to the action space (a set of control actions), for building control [8] - [11]. ETM is also incorporated into mixed-integer programming (MIP)-based optimization for building control [12]. These previous studies demonstrated that the ETM control approach can significantly reduce computation loads as compared to the TTM control approach. However, there are still some research gaps in these previous studies that need to be further investigated. The events in these previous studies were based on the transitions (changes over time) of the current measured building states (e.g., room air temperature and PMV) without considering the past and future building states. As building states are dynamic, events based on only the current measured building states may cause delays in triggering or redundant control/optimization actions, leading to undesirable future building states (e.g., too cool/warm room conditions). Besides, despite the fact that MPC needs to improve its computation efficiency for achieving wide practical applications in buildings, incorporating ETM into MPC to reduce its computation load is still lacking in the literature.

This study proposes an ETMPC, which considers the past, current and future building states in the event space, for optimizing building energy efficiency and thermal comfort. The ETMPC features a novel ETM such that the ETMPC only solves the computation-expensive optimization problem when necessary. The proposed ETM is based on the transition (change over time) of the MPC cost function and captures not only the current but also the past and future building states, which forms the main novelty of this study. A set of simulations based on a test building is conducted to evaluate the control performance of the proposed ETMPC as compared to standard MPC and a conventional thermostat.

2.Methodology

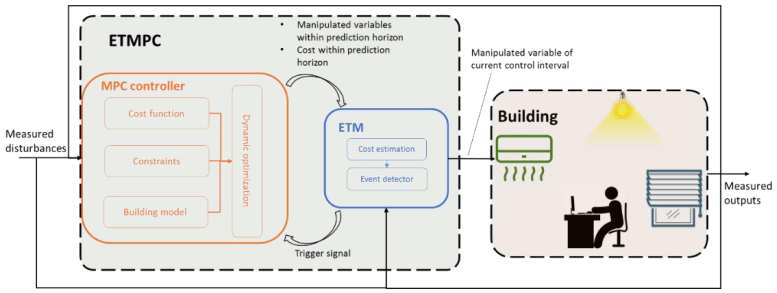

Figure 1. Schematic diagram showing the architecture of the proposed ETMPC.

2.1.Event-triggered model predictive control

Figure 1 shows the architecture of the proposed ETMPC, which consists of a MPC controller, and an ETM. Initially, the MPC controller solves the dynamic optimization problem to generate a sequence of optimal manipulated variables (MVs) (cooling power setpoints for ACMV) for the prediction horizon with the inputs of measured disturbances (MDs) (weather conditions and internal heat loads) and feedback of measured outputs (MOs) (room conditions) of the building. The MPC controller sends the optimal MVs and the corresponding cost (value of the cost function) of the prediction horizon to the ETM. The cost estimation module of the ETM evaluates the transition of the cost based on real-time feedback of MDs and MOs. The event detector module of the ETM detects the occurring of events based on the cost transition. If no event is detected, the ETM sends MV of the current control interval to the building for real-time control. The ETM repeats the process until an event is detected or reaching

the end of the prediction horizon. If an event is detected or the current prediction horizon is finished, the ETM triggers the optimization of the MPC controller and starts a new prediction horizon.

2.2.MPC controller

The objectives of the MPC controller, as described by Equation (1), are to minimize cooling energy consumption, the deviation of indoor PMV from the reference value and the violation of constraints.

$$J = Minimize(\sum_{k=1}^{N} Q_{clg,t+k}/Q_{cc} + \sum_{k=1}^{N}[W_{PMV}(PMV_{t+k} - PMV_{ref})]^2 + W_{\varepsilon}\varepsilon_{t+k}^2), \quad (1)$$

which yields the constraints,

$$0 \le Q_{clg} \le Q_{cc}, -0.5 - \varepsilon \le PMV \le 0.5 + \varepsilon. \quad (2)$$

In Equations (1) and (2), symbols *J*, *Q*, *W*, *PMV*, ε, and *N* refer to objective, heat flow rate (W/m^2), weighting factor, PMV, stack variable and prediction horizon, respectively. Subscripts *t*, *k*, *clg* and *cc* refer to time, index of control intervals in a prediction horizon, cooling and cooling capacity, respectively. Particularly, the three terms on the right side of Equation (1) refer to the costs of cooling energy consumption, thermal discomfort and violation of constraints, respectively. The reference indoor PMV value (PMV_{ref}) is set to be 0, which represents thermal neutrality. The stack variable (ε) softens the constraint of indoor PMV [13] [14]. The weighting factor for indoor PMV (W_{PMV}) is set at 5, which gives a high weightage to the thermal comfort term over other terms in Equation (1), making the MPC controller biased towards tracking the reference PMV rather than minimizing the cooling energy consumption. The control interval and the prediction horizon are set at 5 minutes and 12 control intervals, respectively. The control interval of 5 minutes is fine enough to capture the dynamics of indoor thermal conditions and the prediction horizon of 60 minutes (12 control intervals) is long enough to cover the response time of the indoor thermal conditions.

2.3.Event-triggered mechanism (ETM)

An optimization of the MPC controller generates the optimal MVs for all the control intervals of the prediction horizon. However, in a standard MPC controller, only the MV of the first control interval is applied to real-time building control. To make use of the MVs of remaining control intervals without significantly degrading control performance, an ETM is proposed as described in Figure 2. At time *t*, the MPC controller conducts an optimization and sends the optimal MVs as well as the corresponding cost (c_0) of the objective function (Equation (1)) within the prediction horizon to the ETM. The ETM applies the MV of the first control interval to the building for control. For the subsequent control intervals, the ETM determines whether to apply the MV to the building or to trigger another optimization of the MPC controller based on the transition of the cost. At time *t*+*k*, the ETM re-evaluates the cost (c_k) using the feedback of MOs and MDs within the period of (*t*, *t*+k). The ETM then compares the re-evaluated cost (c_k) and the previous cost (c_0) to calculate the error (*e*) between the two costs according to Equation (3). The ETM evaluates the true/false of an event according to the logic described by Equation (4). If the event is false, the ETM applies the MV of the current control interval (*t*+*k*) to the building for real-time control. If the event is true, the ETM triggers an optimization of the MPC controller to start a new prediction horizon. The process is repeated at each control interval till the end of the prediction horizon when the ETM triggers the optimization action of the MPC controller.

$$e = |c_k - c_0|/c_0. \quad (3)$$

$$event = \begin{cases} true, & e < \delta \\ false, & e \ge \delta \end{cases}, \quad (4)$$

where symbols *e*, *c* and δ refer to error, cost and threshold, respectively.

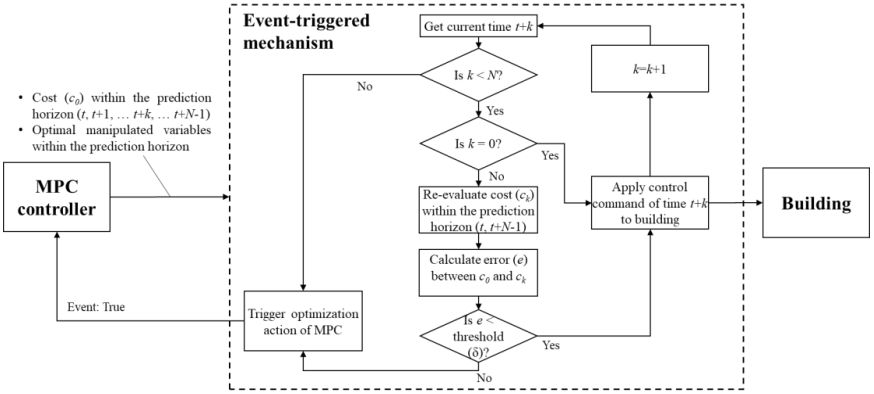

Figure 2. Schematic diagram showing the framework of the proposed ETM.

2.4.Building modelling

In this study, the recurrent neural network (RNN) with nonlinear autoregressive exogenous (NARX) structure, as expressed by Equation (5), is employed to approximate the building dynamics based on data. The NARX RNN is a dynamic network with the feedback of outputs, which is suitable for time-series predictions and, thus, suitable for approximating the dynamics of buildings [15]. The sigmoidal activation function, commonly used for artificial neural networks, is employed in this study. The inputs of the RNN are MVs (cooling power of ACMV) and MDs (weather conditions and internal heat loads), which dominate room conditions. The outputs of the RNN are MOs (indoor PMV). The time delays of the inputs and outputs feedback, as well as the number of neurons in the RNN hidden layer, are determined by the 'trial-and-error' method [14].

$$y_t = f(y_{t-1}, y_{t-2}, \cdots y_{t-n_y}, u_{t-1}, u_{t-2}, \dots u_{t-n_u}) , \quad (5)$$

where symbols *f()*, *y*, *u*, *t* and *n* refer to function, output, input, time and number.

3.Case study

3.1.Test building

The control performance of the proposed ETMPC is evaluated based on Building and Construction Authority (BCA) SkyLab located in Singapore through simulations. A physics-based virtual model of SkyLab developed in the previous study [5] is employed to represent the real building for the simulations. SkyLab has two identical side-by-side cells, Test Cell and Reference Cell. The RNN modelling and simulations in this study are based on Test Cell. Each cell is equipped with eight T5 fluorescent lamp fixtures that provide a lighting load of 8.2 W/m^2 of floor area. Internal sensible load of 16 W/m^2 of floor area and latent load of four persons (55 W per person) are generated by physical load simulators to mimic typical office environments. Test Cell is installed with a fan coil unit (FCU). The chilled water flowrate supplied into the cooling coil of the FCU is regulated by a water valve, which is controlled by a thermostat according to a room air temperature setpoint of 24^{o}C. SkyLab is equipped with an array of sensors in the room space, ACMV system and outdoor space as well as a data acquisition system to monitor real-time room air conditions, ACMV variables and weather conditions. SkyLab and its systems operate from 9 am – 6 pm on weekdays. More details of the test building are described in the previous studies [5].

3.2.Building model

An RNN model, as shown in Figure 3, is developed based on the building operation data of SkyLab Test Cell generated by a simulation with the virtual building model described in Section 3.1. The input data include cooling power provided by the ACMV system (Q_{clg}), outdoor air temperature (T_o), global horizontal irradiance (*GHI*) and the operation status (*os*) (1 – operating, 0 – not operating) of the test

building. *GHI* and T_o represent the disturbances of weather conditions. *os* represents the disturbances of internal heat gains from lighting and load simulators as their operation follows the operation schedule of the test building as described in Section 3.1. The output data include indoor PMV. The clothing insulation and metabolic rate of occupants in the test building are assumed constant at 0.5 clo and 1.2 met per occupant, respectively, for typical office activities and summer season. Singapore typical meteorological year (TMY) data [16] is employed as the weather inputs for the simulation that generates the input/output data for developing the RNN model. The simulation is based on the weather data in April. The heat loads from the lighting system and load simulators are on during operating time and are off during the non-operating time of the test building. The cooling power of the ACMV system is randomly generated between 0% and 100% during the operating time and is 0% during the non-operating time of the test building. The simulated input/output data were divided into three subsets randomly picked across the simulation time, 70% for model training, 15% for model validation and the remaining 15% for model testing. 1:2 of time delays for the inputs and the feedback of outputs as well as 10 neurons in the hidden layer are selected based on the 'trial-and-error' method [14]. The R-values of training, validation and testing phases are 0.986, 0.985 and 0.986.

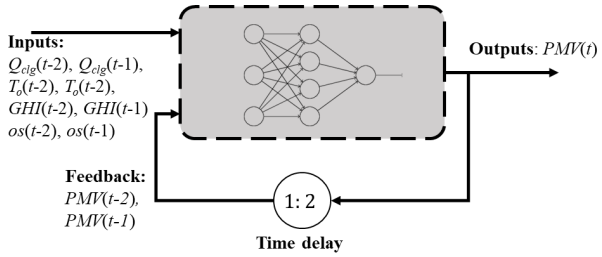

Figure 3. Schematic of the recurrent neural network model of SkyLab Test Cell.

3.3.Simulation setup

To evaluate the control performance of the proposed ETMPC, a set of simulations are conducted including (1) MPC: the formulation is described in Section 2.2 and its optimization action is triggered by TTM. (2) ETMPC: the system architecture is described in Section 2.1. The formulations of its MPC controller and ETM are described in Sections 2.2 and 2.3. Various settings of δ including (0.5%, 1%, 1.5%, 3%, 4.5%, 6%, 7.5%, 9%, 10.5%, 12%, 13.5%, 15%, 16.5%, 18%, 19.5%, 21%, 22.5%, 24%) are tested; (3) Thermostat: on/off control based on the feedback of room air temperature to represent conventional reactive control. The lower and upper bounds of temperature for the on (i.e. cooling power is 100%) and off (i.e. cooling power is 0%) actions are 23ºC and 25ºC, respectively. This kind of thermostat is a common practice in current buildings. The comparison of MPC and proportional-integral (PI) control can be found in the previous study [13]. Singapore TMY data [16] is employed as the weather inputs for the simulations. The simulations are conducted based on the weather data in May. The thermal comfort performance is evaluated using a thermal discomfort index (TDI) defined by Equation (6). Energy consumption performance is evaluated using the electricity consumption due to cooling based on the coefficient of performance (COP) of 5.87 of the chiller serving the test building.

$$TDI = \left[\int_{t=0}^{t_{sim}} os * \left(\left|PMV(t) - PMV_{ref}(t)\right|\right)\right] / \left[\int_{t=0}^{t_{sim}} os\right], \quad (6)$$

where subscript *sim* refers to simulation. Particularly, variable t_{sim} refers to the total time of the simulation period.

3.4.Results and discussion

3.4.1.Results on a typical day. Figure 4 shows the optimization actions (0 – false, 1 – true) of MPC and ETMPC (δ = 1.5%) plotted in stair-step graph on a typical day during 9 am – 6 pm. The optimization of the MPC was triggered at each control interval along the day due to its TTM. However, the number of optimization actions was largely reduced by the ETMPC due to its ETM as described in Section 2.3. Compared to MPC that only applies the MV at the first control interval of the prediction horizon to real-time building control, the ETMPC also makes use of the MVs of the remaining control intervals as long

as the error of cost (Equation (3)) is below the threshold (δ = 1.5%). The results in Figure 4 suggest that the ETMPC can significantly improve the computation efficiency as compared to MPC by largely reducing the number of optimization actions.

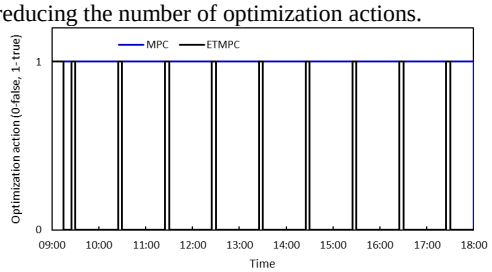

Figure 4. Stair-step plot of the optimization actions (0 – false, 1 – true) of MPC and ETMPC (δ = 1.5%) on a typical day.

Figure 5 shows the time series plots of indoor PMV and normalized cooling power (Q_{clg}/Q_{cc}) of the thermostat, MPC and ETMPC on the same day as Figure 4. Figure 5 (a) shows that the thermostat kept indoor PMV in a fluctuating manner due to its reactive control nature. The thermostat also kept indoor PMV below the comfortable range (-0.5, 0.5) sometimes. In contrast, the MPC achieved much better indoor PMV as compared to the thermostat by keeping indoor PMV close to the thermal neutrality (PMV = 0) throughout the day except for the ACMV start-up time period in the morning. The ETMPC also maintained indoor PMV close to thermal neutrality (PMV = 0) similar to the MPC does except for the time around 9:50 am when indoor PMV of ETMPC was differing a bit (around 0.03) from that of MPC. Figure 5 (b) shows the normalized cooling power results of the three controllers. The thermostat regulates cooling power between 0% and 100%, echoing the indoor PMV results in Figure 5 (a).

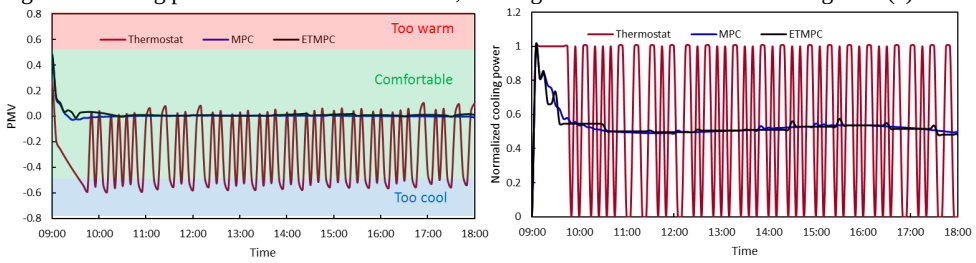

(a) (b)

Figure 5. Time series plots of (a) indoor PMV and (b) normalized cooling power of thermostat, MPC and ETMPC (δ =1.5%) on a typical day.

3.4.2.Results in the whole simulation period. Figure 6 shows the overall numbers of optimization actions of MPC and ETMPCs with various values of δ. The MPC case is represented by ETMPC with δ of 0, as they are essentially the same. Figure 6 shows that ETMPC (δ > 0 in Figure 6, same for the remaining content of the paper) significantly reduced the number of optimization actions of MPC (δ = 0 in Figure 6, same for the remaining content of the paper) from 2484 times to 557 – 293 times, i.e. percentage reduction of 77.6% - 88.2%. The reduction of optimization actions is slightly higher when δ increases. When δ is larger than 19.5%, the number of optimization actions does not reduce further. The large reduction of optimization actions by ETMPC compared to MPC can cut the computing power demand (i.e., expensive hardware) of MPC, which is a major limitation of MPC. Hence, ETMPC can largely improve the potential of practical building applications of MPC.

Figure 7 shows the energy performance of the MPC and ETMPC. Figure 7 (a) shows the electricity consumption due to the cooling of the MPC and ETMPCs with various δ values. The MPC consumed 168.7 kWh in the simulation period. It was slightly reduced by ETMPC to 168.0 – 168.1 kWh. The change of δ value doesn't affect the energy consumption of ETMPC obviously. Figure 7 (b) shows the percentage energy savings of MPC and ETMPCs with various δ values as compared to the thermostat. The thermostat consumed 185.3 kWh of electricity in the simulation period. It shows that the MPC reduced 9% energy saving and the ETMPC achieved 9.3% - 9.4% energy savings as compared to the thermostat. The results in Figure 7 suggest that the ETM doesn't degrade the energy performance of MPC, instead, improves it a bit.

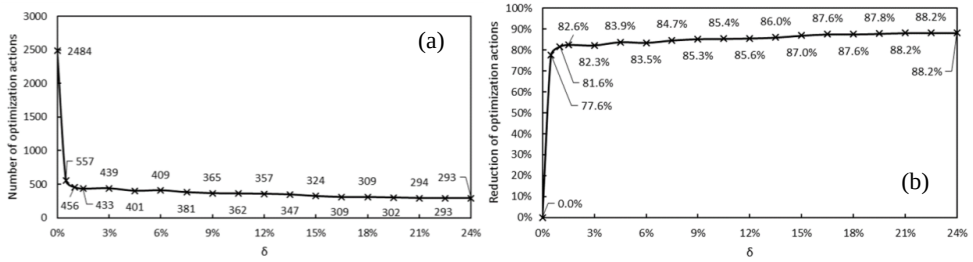

Figure 6. Optimization actions of MPC and ETMPCs with various values of δ. (a) number of optimization actions, (b) reduction of optimization actions as compared to MPC.

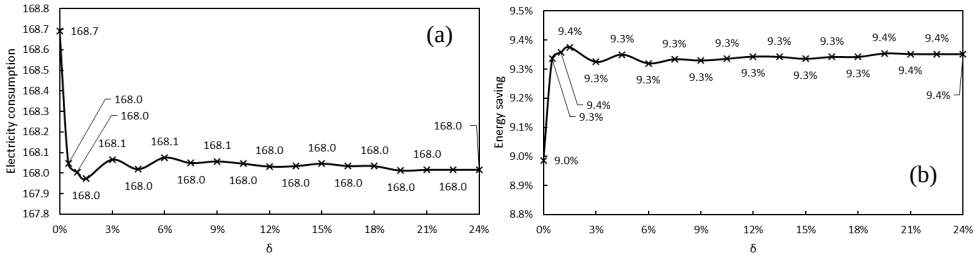

Figure 7. Energy performance of MPC and ETMPCs with various values of δ. (a) electricity consumption, (b) energy savings compared to the thermostat.

Figure 8 shows the thermal comfort results of MPC and ETMPC. Figure 8 (a) shows the TDI of the MPC and ETMPCs with various δ values. It shows that the TDI increases slightly, i.e. thermal comfort performance decreases, with the increase of δ. However, when δ is larger than 3%, the TDI of the ETMPC does not increase much further. Figure 8 (b) shows the percentage improvement of TDI of the MPC and ETMPCs as compared to the thermostat. The TDI of the thermostat is 0.325 during the simulation period. The MPC reduced the TDI by 85.8% and the ETMPC reduced the TDI by 79.4% - 82.9% as compared to the thermostat. The results in Figure 8 suggest that the thermal comfort performance of ETMPC is reduced as compared to the MPC but is still much better than the thermostat and reduction is minor and imperceptible. Hence this setback of ETMPC is trivial considering the large computational efficiency improvement (77.6% - 88.2%) by ETMPC as compared to MPC, which can largely cut down the computing power demand for MPC.

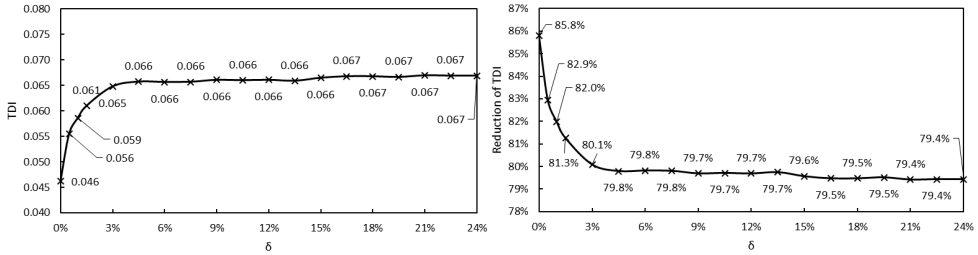

(a) (b)

Figure 8. Thermal comfort performance of MPC and ETMPC with various values of δ. (a) TDI, (b) reduction of TDI compared to the thermostat.

4.Conclusion

This study proposed an ETMPC for optimizing building energy efficiency and thermal comfort. The ETMPC features an ETM, which conducts the optimization only when it is needed. The control performance of the ETMPC is evaluated and compared to a thermostat and a MPC through a set of simulations. Based on the simulation results, it can be concluded that (1) the ETMPC can significantly improve the computation efficiency by 77.6% - 88.2% as compared to the MPC; (2) with the

improvement of computation efficiency, the ETMPC does not degrade the energy performance (3) with the significant improvement of computation efficiency, the ETMPC only degrades the thermal comfort performance slightly as compared to the MPC; (4) the thermal comfort and computation efficiency performance of the ETMP is slightly degraded with the increase of the threshold to determine the event but keeps constant when the threshold is larger than a certain value.

Acknowledgement
This research is supported JTC Corporation (contract nos. N190107T00 and 2019-0607) and Smart Nation & Digital Government Office of Singapore (Grant no. NRF2016IDM-TRANS001-031).

Reference
[1] Graus W, Blomen E and Worrell E 2011 Global energy efficiency improvement in the long term: a demand-and supply-side perspective. Energy Efficiency, 4(3), 435-63.
[2] Krarti M, Dubey K and Howarth N 2019 Energy productivity analysis framework for buildings: a case study of GCC region. Energy, 167, 1251-65.
[3] Shaikh P H, Nor N B M Nallagownden P, Elamvazuthi I and Ibrahim T 2014 A review on optimized control systems for building energy and comfort management of smart sustainable buildings. Renewable and Sustainable Energy Reviews, 34, 409-29.
[4] Chua K J, Chou S K, Yang W M and Yan J 2013 Achieving better energy-efficient air conditioning–a review of technologies and strategies. Applied Energy, 104, 87-104.
[5] Yang S, Wan M P, Ng B F, Zhang T, Babu S, Zhang Z, Chen W and Dubey S 2018 A state-space thermal model incorporating humidity and thermal comfort for model predictive control in buildings. Energy and Buildings, 170, 25-39.
[6] Yang S, Wan M P, Ng B F, Zhang Z, Lamano A S and Chen W 2018 Modeling and model calibration for model predictive occupants comfort control in buildings. In Proceedings of 7th International Building Physics Conference 2018.
[7] Yang S, Uthayakumar N, Yeo W J and Wan M P 2021 Machine-Learning-Based Model Predictive Control with Instantaneous Linearization for Building Energy Management. IEEE 5th International Conference on Green Energy and Applications. (In press).
[8] Wang J, Jia Q S, Huang G and Sun Y 2018 Event-driven optimal control of central air-conditioning systems: Event-space establishment. Science and Technology for the Built Environment, 24(8), 839-849.
[9] Sun B, Luh P B, Jia Q S and Yan B 2015 Event-based optimization within the Lagrangian relaxation framework for energy savings in HVAC systems. IEEE Transactions on Automation Science and Engineering, 12(4), 1396-1406.
[10] Jia Q S, Wu J, Wu Z and Guan X 2018. Event-based HVAC control—a complexity-based approach. IEEE Transactions on Automation Science and Engineering, 15(4), 1909-19.
[11] Hosseinloo A H, Ryzhov A, Bischi A, Ouerdane H, Turitsyn K and Dahleh M A 2020 Data-driven control of micro-climate in buildings: An event-triggered reinforcement learning approach. Applied Energy, 277, 115451.
[12] Xu Z, Hu G, Spanos C J and Schiavon S 2017 PMV-based event-triggered mechanism for building energy management under uncertainties. Energy and Buildings, 152, 73-85.
[13] Yang S, Wan M P, Ng B F, Dubey S, Henze G P, Rai S K and Baskaran K 2019 Experimental study of a model predictive control system for active chilled beam (ACB) air-conditioning system. Energy and Buildings, 203, 109451.
[14] Yang S, Wan M P, Chen W, Ng B F and Dubey S 2021. Experiment study of machine-learning-based approximate model predictive control for energy-efficient building control. Applied Energy, 288, 116648
[15] Katić K, Li R, Verhaart J and Zeiler W 2018. Neural network based predictive control of personalized heating systems. Energy and Buildings, 174, 199-213.
[16] ASHRAE 2001 IWEC:User's Manual and CD-ROM, ASHRAE.